PARAFAC-PARATUCK Semi-Blind Receivers for Two-Hop Cooperative MIMO Relay Systems

Leandro R. Ximenes, Gérard Favier, André L. F. de Almeida, *Senior Member, IEEE* and Yuri C. B. Silva

***Abstract*—In two-hop amplify-and-forward (AF) relay systems, a source node sends information to one or several relay nodes that amplify and retransmit the received signals to a destination node, without decoding. Such AF relaying-based cooperative communications allow to improve communication reliability due to increased channel gains and space diversity at the destination node. In this paper, we consider a two-hop AF cooperative scheme, with a simplified Khatri-Rao space-time (KRST) coding at transmission (source). We show that the third-order tensor of signals received by the destination node satisfies a PARAFAC decomposition for the direct link, and a PARATUCK2 decomposition for the relay-assisted link. This tensorial modeling enables a joint semi-blind estimation of transmitted symbols and channels of both hops. Three receivers that combine these two tensor models in different ways are proposed. An identifiability study for these receivers is carried out, from which sufficient conditions for joint symbol and channel recovery are derived. The performance of these receivers is illustrated by means of simulation results, and a comparison is made with recent supervised approaches that allow to estimate channels and symbols in two separated steps. Besides a joint semi-blind channel/symbol estimation, our approach gives a better BER performance due to coding at the transmitter.**

***Index Terms*—Cooperative communications, channel estimation, MIMO systems, PARAFAC, PARATUCK2, space-time coding, symbol estimation, semi-blind estimation.**

I. Introduction

In cooperative communications, two or more transmit nodes are combined to increase diversity and/or signal power at the receiver. Such communications can be viewed as several single-antenna nodes functioning as a virtual array of multiple antennas, or as a system using relay stations that simply forward amplified signals in areas of low coverage in mobile telephony. Cooperative communications are now an important research field [1]–[3], and the adoption of relay stations has been commonly accepted as a key technique for improving the link performance of future wireless communication systems [4], [5]. For such relay-assisted systems, multiple links including mobile terminals to a base station, mobile terminals to relay stations and relay stations to a base station are used to create a virtual multiple input multiple output (MIMO) system [6], [7].

Relaying strategies are classified according to the forwarding protocol (i.e. amplify-and-forward (AF), decode-and-forward (DF) and others), and also to the network topology (i.e. one-way and two-way) [8]–[10]. Among the existing schemes, two-hop relaying is well known as an efficient way to extend coverage area and to overcome impairments such as fading, shadowing, and path loss, in wireless channels [6]. When the direct links between the sources (co-channel users) and the destination (base station) are deeply faded, relay stations are used to improve the communication.

In this work, we consider a two-hop AF relaying system due to its simplicity of implementation. More specifically, we consider a scenario where i) a multiple-antenna source node communicates with a multiple-antenna relay in the first hop (source to relay (SR) link); ii) the relay communicates with a multiple-antenna destination node in the second hop (relay to destination (RD) link); iii) a direct link between the source and destination nodes (herein called source to destination (SD) link) may be available. We are interested in a scenario where channel state information (CSI) is available neither at the relay nor at the destination. Concerning the network topology, this work focuses on a one-way half-duplex relaying scenario, where the information is transmitted from the source to the destination during two consecutive transmission phases.

With the aim of simplifying the computational burden at the relay stations, a receiver algorithm is used at the destination only. In the context of two-hop relaying systems, the reliability of receivers strongly depends on the accuracy of CSI for both SR and RD links. Moreover, the use of precoding techniques at the source and/or the relay generally requires the instantaneous CSI knowledge of both hops to carry out transmit optimization [11]–[14]. However, in real-life communication systems, the CSI is unknown, and therefore, has to be estimated. Conventional point-to-point pilot-based strategies do not provide channel estimation of both hops separately at the destination. The approach considered in this work aims to jointly estimate the transmitted symbols and the aforementioned channels, with a reduced computational complexity at the relay station.

Recently, tensor analysis has shown to be an efficient approach for channel estimation and/or symbol detection in cooperative diversity systems [15]–[18]. Although these works consider different relay processing schemes, their common feature is the use of the parallel factor (PARAFAC) decomposition [19], [20], for modeling either the relay processing (as in [15], [16]) or the received signals (as in [17], [18]). For point-to-point (non-cooperative) multiple-antenna communication systems, tensor-based methods have been proposed in a number of works [21]–[25] to solve the problem of blind/semi-blind channel and symbol estimation by exploiting several diversities (e.g. space, time, frequency and/or code). According to these works, the different ways of designing the transmitter lead to different tensor models for the received signals

Leandro R. Ximenes and Gérard Favier are with the I3S Laboratory, University of Nice-Sophia Antipolis (UNS), CNRS, France. (e-mail: ximenes@i3s.unice.fr; favier@i3s.unice.fr). André L. F. de Almeida and Yuri C. B. Silva are with the Wireless Telecom Research Group, Department of Teleinformatics Engineering, Federal University of Ceará, Fortaleza, Brazil. (e-mail: andre@gtel.ufc.br; yuri@gtel.ufc.br). This work was partially supported by CNPq and FUNCAP.

(e.g. PARAFAC, CONFAC, PARATUCK2 and PARATUCK-(2,4)), each system having its own identifiability properties. The tensor-based receivers developed in these works allow a joint symbol and channel estimation under more relaxed conditions than matrix-based methods and without requiring pilot sequences for CSI acquisition.

However, very few works propose tensor-based receivers for cooperative communications. Besides, the few studies concerning tensor modeling of cooperative MIMO systems usually focus on the problem of channel estimation. For instance, in [15] and [16], a tensorial formulation is applied to two-way MIMO relaying systems. In these works, training sequences are used for channel estimation, which is achieved by firstly canceling self-interference, and then using algebraic refinement steps. In [18], the authors develop a training based technique for channel estimation in MIMO relay systems using PARAFAC analysis. The approach proposed therein allows a simultaneous estimation of the SR and RD channels at the destination node using an alternating least squares (ALS) algorithm, and without the need of any complex processing at the relay. It is shown that PARAFAC-based channel estimation can provide a more accurate channel estimation in comparison with the two-stage training method proposed in [26], especially at high signal to noise ratio (SNR) levels. With the idea of avoiding the use of training sequences at the source, the work [17] proposes a blind receiver for uplink multiuser cooperative diversity systems employing an antenna array at the base station. The idea was to explicitly incorporate "cooperation" as the third diversity dimension of the received data, in addition to space (receive antennas) and time (symbol periods) dimensions.

This work proposes a new tensor-based approach for joint semi-blind symbol and channel estimation in two-hop AF MIMO relay-assisted systems. We consider a transmission scheme known as Khatri-Rao space-time (KRST) coding [27] at the source node, combined with an AF coding scheme at the relay node. We show that the third-order tensor of signals received by the destination node satisfies a PARAFAC decomposition for the direct (SD) link, and a PARATUCK2 decomposition for the relay-assisted (SR-RD) link, herein denoted the source-relay-destination (SRD) link. Such a hybrid tensorial modeling enables a semi-blind estimation of symbols and channels of both hops at the destination only, without requiring training sequences, and alleviating the computational complexity at the relay node. We propose three receiver algorithms that are based on different combinations of both SD and SRD links, namely:

- *PARATUCK2*: baseline approach, where the link SD is not used, i.e. symbol and channel estimation is based only on the SRD link;
- *Sequential PARAFAC/PARATUCK2 (SPP)*: a PARAFAC-based estimation using the SD link provides symbol estimates that are used to initialize the PARATUCK2-based algorithm that operates on the SRD link;
- *Combined PARAFAC/PARATUCK2 (CPP)*: both links are combined by means of a hybrid PARAFAC-PARATUCK2 estimator of the transmitted symbols, while the estimated channel of the link SD is updated at each iteration.

An identifiability study for the proposed receivers is also carried out. The derived identifiability conditions provide a guideline for choosing the relevant system parameters (code length and numbers of antennas at the source, relay and destination) that guarantee symbol and/or channel recovery.

If one considers only the relay-assisted link, the proposed PARAFAC-PARATUCK2 receiver can be viewed as an alternative to the PARAFAC receiver derived in [18] without the need of using training sequences. Indeed, in our approach, the source node applies space-time coding instead of sending training sequences to the relay and destination. By simultaneously using the SD and SRD links, i.e. by combining the PARAFAC and PARATUCK2 tensor models in different ways, the proposed receivers generalize the one of [18] . Note that in [18], although the link SD is assumed to be available, it is not exploited for channel estimation using the SRD link. In this work, we show that the SD link can indeed be integrated into the iterative estimation process along with the SRD link for improving symbol estimation, with the advantage of avoiding training sequences. When compared with supervised methods [18], [28], both CPP and SPP receivers provide a slightly worse channel estimation, but a considerably better symbol estimation accuracy, leading to lower error rates due to the KRST coding used at the source. Assuming that the energy of the signal received through the link SD is not negligible[1], our results show that the SPP and CPP algorithms offer a faster convergence and better symbol estimates than the PARATUCK2 algorithm that does not exploit the SD link. Furthermore, the BER performance gain of the CPP receiver over the SPP one corroborates the increase of spatial diversity when combining both links for symbol estimation.

The rest of this paper is organized as follows. In Section II, the notations are defined and some properties are recalled. In Section III, the system model is described. The tensor models of signals received via the direct and relay-assisted links are presented by resorting to PARAFAC and PARATUCK2 decompositions, respectively. In Section IV, three iterative receiver algorithms are formulated. Identifiability issue is also discussed. Simulation results are presented in Section V and the paper is concluded in Section VI.

II. NOTATIONS

Scalars, column vectors, matrices, and tensors are denoted by lower-case $(a, b, \ldots)$, boldface lower-case $(\mathbf{a}, \mathbf{b}, \ldots)$, boldface capital $(\mathbf{A}, \mathbf{B}, \ldots)$, and calligraphic $(\mathcal{A}, \mathcal{B}, \ldots)$ letters, respectively.

$\mathbf{A}^T$, $\mathbf{A}^H$, $\mathbf{A}^\dagger$, $\mathbf{A}_{l.}$, and $\mathbf{A}_{.m}$ are the transpose, the Hermitian transpose, the Moore-Penrose pseudo-inverse, the l^{th} row and the m^{th} column of $\mathbf{A} \in \mathbb{C}^{L \times M}$, respectively, and $\|.\|_F$ denotes the Frobenius norm. The term $diag(\mathbf{b})$ refers to the diagonal matrix with the vector $\mathbf{b}$ forming its diagonal, whereas $D_n(\mathbf{B})$ corresponds to the diagonal matrix with the n^{th} row of $\mathbf{B}$ forming its diagonal, so $D_n(\mathbf{B}) = diag(\mathbf{B}_{n.})$. The operator vec(.) vectorizes its matrix argument by stacking its columns.

[1]In this scenario, the AF relay-assisted link aims to help the source to communicate with the destination by increasing the signal power at the receiver in areas of limited coverage while providing additional spatial diversity.

$\otimes$ and $\diamond$ denote the Kronecker and the Khatri-Rao (column-wise Kronecker) matrix products, respectively. For $\mathbf{A} \in \mathbb{C}^{L\times M}$ and $\mathbf{B} \in \mathbb{C}^{N\times M}$, we have

$$\begin{aligned}\mathbf{A}\diamond\mathbf{B} &= \begin{bmatrix} \mathbf{B}D_1(\mathbf{A}) \\ \vdots \\ \mathbf{B}D_L(\mathbf{A}) \end{bmatrix} \in \mathbb{C}^{NL\times M} \\ &= [\mathbf{A}_{\cdot 1}\otimes\mathbf{B}_{\cdot 1},\ \cdots,\ \mathbf{A}_{\cdot M}\otimes\mathbf{B}_{\cdot M}],\end{aligned} \tag{1}$$

The two following properties are used in this work

$$\text{vec}\left(\mathbf{A}\mathbf{B}\mathbf{C}^T\right) = (\mathbf{C}\otimes\mathbf{A})\text{vec}(\mathbf{B}) \tag{2}$$

$$\text{vec}\left(\mathbf{A}D_n(\mathbf{B})\mathbf{C}^T\right) = (\mathbf{C}\diamond\mathbf{A})\,\mathbf{B}_{n\cdot}^T. \tag{3}$$

Given a third-order tensor $\mathcal{A} \in \mathbb{C}^{I\times J\times K}$, with entry $a_{i,j,k}$, the so-called horizontal, lateral and frontal slices are denoted by $\mathbf{A}_{i\cdot\cdot} \in \mathbb{C}^{J\times K}$, $\mathbf{A}_{\cdot j\cdot} \in \mathbb{C}^{K\times I}$ and $\mathbf{A}_{\cdot\cdot k} \in \mathbb{C}^{I\times J}$, respectively. The i^{th} horizontal slice is obtained by fixing the (first-mode) index i of $\mathcal{A}$, and varying j and k. Three matrix representations of $\mathcal{A}$ corresponding to mode-1, mode-2 and mode-3 unfoldings, are denoted $\mathbf{A}_{JK\times I}$, $\mathbf{A}_{KI\times J}$ and $\mathbf{A}_{IJ\times K}$, with

$$\begin{aligned}a_{i,j,k} &= [\mathbf{A}_{JK\times I}]_{(k-1)J+j,i} = [\mathbf{A}_{KI\times J}]_{(i-1)K+k,j} \\ &= [\mathbf{A}_{IJ\times K}]_{(j-1)I+i,k}\,.\end{aligned}$$

III. System model

Let us consider a two-hop one-way cooperative scheme with a source (S) node, a destination (D) node and a relay (R), as illustrated by Fig. 1, where M_S, M_D, and M_R denote the numbers of antennas at the source, the destination, and the relay, respectively, while $\mathbf{H}^{(SD)} \in \mathbb{C}^{M_D\times M_S}$, $\mathbf{H}^{(SR)} \in \mathbb{C}^{M_R\times M_S}$ and $\mathbf{H}^{(RD)} \in \mathbb{C}^{M_D\times M_R}$ are the channel of the direct link to destination (SD link), and the channels between the source and the relay (SR link), and between the relay and the destination (RD link), respectively. All these channels are assumed to be constant during the total transmission time divided into two phases (two hops). During the first one, the source transmits the information signals to the relay and also to the destination through the SR and SD links, respectively. During the second one, the source stays silent, and the relay forwards the amplified signals to the destination. In other words, this half-duplex scheme forces the relay to store all transmitted information before forwarding it. Duplex schemes enable immediate forwarding (no storage), but with a greater difficulty of practical implementation.

Let $\mathbf{S} \in \mathbb{C}^{N\times M_S}$ be the matrix containing the information symbols multiplexed to the M_S antennas during N time-blocks. A simplified KRST coding (without precoding) [27] characterized by the code matrix $\mathbf{C} \in \mathbb{C}^{P\times M_S}$, is used in order to introduce time redundancy

$$\mathbf{X}_n = D_n(\mathbf{S})\mathbf{C}^T \in \mathbb{C}^{M_S\times P},$$

where P is the number of symbol periods contained in each time-block. In other words, each phase corresponds to the transmission of a block of NM_S symbols during a transmission time of PN symbol periods.

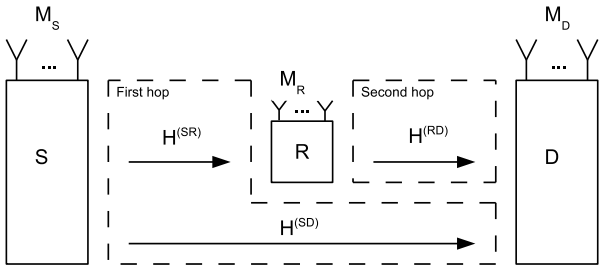

Fig. 1. Two-hop one-way scheme

A. Model of the direct link (SD)

Considering the n^{th} time-block of the first phase of the protocol, the signals received at destination via the direct link are stored in the n^{th} frontal slice $\mathbf{Y}_{\cdot\cdot n}^{(SD)}$ of the third-order received signal tensor $\mathcal{Y}^{(SD)} \in \mathbb{C}^{M_D\times P\times N}$, defined as

$$\begin{aligned}\mathbf{Y}_{\cdot\cdot n}^{(SD)} &= \mathbf{H}^{(SD)}\mathbf{X}_n \in \mathbb{C}^{M_D\times P} \\ &= \mathbf{H}^{(SD)}D_n(\mathbf{S})\mathbf{C}^T,\end{aligned} \tag{4}$$

Equation (4) represents a PARAFAC decomposition ([19], [29]) of the tensor $\mathcal{Y}^{(SD)}$, with $\mathbf{S}$, $\mathbf{C}$ and $\mathbf{H}^{(SD)}$ as matrix factors. Each entry of $\mathcal{Y}^{(SD)}$ is given by

$$y_{m_D,p,n}^{(SD)} = \sum_{m_S=1}^{M_S} h_{m_D,m_S}^{(SD)} c_{p,m_S} s_{n,m_S}.$$

The mode-1, mode-2 and mode-3 unfolded forms of this PARAFAC model are given, respectively, by

$$\mathbf{Y}_{PN\times M_D}^{(SD)} = (\mathbf{S}\diamond\mathbf{C})\left(\mathbf{H}^{(SD)}\right)^T, \tag{5}$$

$$\mathbf{Y}_{NM_D\times P}^{(SD)} = (\mathbf{H}^{(SD)}\diamond\mathbf{S})\mathbf{C}^T \tag{6}$$

and

$$\mathbf{Y}_{M_DP\times N}^{(SD)} = \left(\mathbf{C}\diamond\mathbf{H}^{(SD)}\right)\mathbf{S}^T. \tag{7}$$

Applying property (3) to (4), we obtain a vectorized form of $\mathbf{Y}_{\cdot\cdot n}^{(SD)}$

$$\mathbf{y}_n^{(SD)} = (\mathbf{C}\diamond\mathbf{H}^{(SD)})\mathbf{s}_n \in \mathbb{C}^{M_DP\times 1}, \tag{8}$$

where $\mathbf{s}_n = \mathbf{S}_{n\cdot}^T \in \mathbb{C}^{M_S\times 1}$, and (8) is the n^{th} column of the mode-3 unfolded form (7) of $\mathcal{Y}^{(SD)}$.

B. Model of the link via relay (SRD)

During the first phase, the coded signals are also transmitted to the relay through the channel $\mathbf{H}^{(SR)} \in \mathbb{C}^{M_R\times M_S}$. The signals received at the relay are stored in a third-order tensor $\mathcal{R} \in \mathbb{C}^{M_R\times P\times N}$ whose n^{th} frontal slice is given by

$$\begin{aligned}\mathbf{R}_{\cdot\cdot n} = \mathbf{R}_n &= \mathbf{H}^{(SR)}\mathbf{X}_n \in \mathbb{C}^{M_R\times P} \\ &= \mathbf{H}^{(SR)}D_n(\mathbf{S})\mathbf{C}^T.\end{aligned}$$

These signals are coded by means of an AF matrix $\mathbf{G} \in \mathbb{C}^{N\times M_R}$

$$\begin{aligned}\bar{\mathbf{R}}_n &= D_n(\mathbf{G})\mathbf{R}_n \in \mathbb{C}^{M_R\times P} \\ &= D_n(\mathbf{G})\mathbf{H}^{(SR)}D_n(\mathbf{S})\mathbf{C}^T,\end{aligned}$$

and then sent from the relay to the destination node during the second phase, through the channel $\mathbf{H}^{(RD)} \in \mathbb{C}^{M_D \times M_R}$. The diagonal matrix $D_n(\mathbf{G})$ contains the AF coefficients applied at the relay during the n-th time-block. It is assumed that each time-block is associated with a different set of coefficients. Such a time-varying AF coding scheme has also been used in some recent works ([16], [18], [28], [30]) for channel estimation purposes using pilot signals. The signals received at destination form a third-order tensor $\mathcal{Y}^{(SRD)} \in \mathbb{C}^{M_D \times P \times N}$ whose n^{th} frontal slice is given by

$$\begin{aligned}\mathbf{Y}_{..n}^{(SRD)} &= \mathbf{H}^{(RD)}\bar{\mathbf{R}}_n \in \mathbb{C}^{M_D \times P} \\ &= \mathbf{H}^{(RD)} D_n(\mathbf{G}) \mathbf{H}^{(SR)} D_n(\mathbf{S}) \mathbf{C}^T. \end{aligned} \quad (9)$$

This equation corresponds to a PARATUCK2 decomposition ([31]) of the tensor $\mathcal{Y}^{(SRD)}$, with $\mathbf{H}^{(RD)}$ and $\mathbf{C}$ as matrix factors, $\mathbf{H}^{(SR)}$ as the core matrix, and $\mathbf{G}$ and $\mathbf{S}$ as interaction matrices. This decomposition can be rewritten in scalar form as

$$y_{m_D,p,n}^{(SRD)} = \sum_{m_R=1}^{M_R} \sum_{m_S=1}^{M_S} h_{m_D,m_R}^{(RD)} g_{n,m_R} h_{m_R,m_S}^{(SR)} s_{n,m_S} c_{p,m_S}.$$

Both PARAFAC and PARATUCK2 decompositions are essentially unique under some mild conditions, which allows a semi-blind joint estimation of channel and symbol matrices. In the following, we present some vectorized and unfolded forms of the tensor $\mathcal{Y}^{(SRD)}$ in order to estimate the channel ($\mathbf{H}^{(SR)}$, $\mathbf{H}^{(RD)}$) and symbol ($\mathbf{S}$) matrices by means of an alternating least squares (ALS) algorithm. A complete demonstration of the following equations can be found in Appendix A.

The vectorized form $\mathbf{y}^{(SRD)} \in \mathbb{C}^{M_D PN \times 1}$ that will be used to estimate $\mathbf{h}^{(SR)} = vec(\mathbf{H}^{(SR)})$ is given by

$$\mathbf{y}^{(SRD)} = \mathbf{W}_1 \mathbf{h}^{(SR)}, \quad (10)$$

with

$$\mathbf{W}_1 = \left(\mathbf{S}^T \diamond \mathbf{G}^T\right)^T \diamond \left(\mathbf{C} \otimes \mathbf{H}^{(RD)}\right) \in \mathbb{C}^{M_D PN \times M_R M_S}. \quad (11)$$

In order to estimate the channel $\mathbf{H}^{(RD)}$, we use the mode-1 unfolded form $\mathbf{Y}_{PN \times M_D}^{(SRD)}$ of $\mathcal{Y}^{(SRD)}$, given by

$$\mathbf{Y}_{PN \times M_D}^{(SRD)} = \mathbf{W}_2 \left(\mathbf{H}^{(RD)}\right)^T, \quad (12)$$

where

$$\mathbf{W}_2 = (\mathbf{I}_N \otimes \mathbf{C})\mathbf{F} \in \mathbb{C}^{PN \times M_R} \quad (13)$$

and

$$\mathbf{F} = \begin{bmatrix} D_1(\mathbf{S}) \left(\mathbf{H}^{(SR)}\right)^T D_1(\mathbf{G}) \\ \vdots \\ D_N(\mathbf{S}) \left(\mathbf{H}^{(SR)}\right)^T D_N(\mathbf{G}) \end{bmatrix} \in \mathbb{C}^{M_S N \times M_R}. \quad (14)$$

The symbol matrix $\mathbf{S}$ can be estimated row by row (i.e. by estimating $\mathbf{s}_n = \mathbf{S}_{n.}^T$ for each n) using the relay-assisted link. Property (3) applied to (9) gives

$$\mathbf{y}_n^{(SRD)} = \mathbf{W}_3 \mathbf{s}_n \in \mathbb{C}^{M_D P \times 1}, \quad (15)$$

where

$$\mathbf{W}_3 = \mathbf{C} \diamond \mathbf{Z}_n^{(SRD)} \in \mathbb{C}^{M_D P \times M_S} \quad (16)$$

and

$$\mathbf{Z}_n^{(SRD)} = \mathbf{H}^{(RD)} D_n(\mathbf{G}) \mathbf{H}^{(SR)} \in \mathbb{C}^{M_D \times M_S}. \quad (17)$$

$\mathbf{Z}_n^{(SRD)}$ can be interpreted as the effective channel of the SRD link during the n^{th} time-block.

In next section, we show how the channel and symbol matrices of the proposed cooperative MIMO system can be jointly estimated using ALS type algorithms. We also discuss the uniqueness properties of the PARAFAC and PARATUCK2 models.

IV. Symbol and Channel Estimation

In this section, we propose three different receivers to estimate the system parameters. These receivers combine differently the tensor models (PARAFAC and PARATUCK2) previously presented.

Let us define

$$\begin{aligned}\widetilde{\mathcal{Y}}^{(SD)} &= \mathcal{Y}^{(SD)} + \mathcal{V}^{(SD)} \\ \widetilde{\mathcal{R}} &= \mathcal{R} + \mathcal{V}^{(R)} \\ \widetilde{\mathcal{Y}}^{(SRD)} &= \mathcal{Y}^{(SRD)} + \mathcal{V}^{(SRD)}\end{aligned}$$

where $\mathcal{V}^{(SD)} \in \mathbb{C}^{M_D \times P \times N}$ and $\mathcal{V}^{(R)} \in \mathbb{C}^{M_R \times P \times N}$ are additive white Gaussian noise tensors at the destination and relay nodes, respectively, while $\mathcal{V}^{(SRD)} \in \mathbb{C}^{M_D \times P \times N}$ contains both the additive white Gaussian noise $\mathcal{V}^{(D)} \in \mathbb{C}^{M_D \times P \times N}$ at destination and the noise $\mathcal{V}^{(R)} \in \mathbb{C}^{M_R \times P \times N}$ amplified by the gain $\mathbf{G}$ and filtered by the channel $\mathbf{H}^{(RD)}$, so that we have

$$\mathbf{V}_{..n}^{(SRD)} = \mathbf{H}^{(RD)} D_n(\mathbf{G}) \mathbf{V}_{..n}^{(R)} + \mathbf{V}_{..n}^{(D)}.$$

A. Direct link: SVD-based receiver (PARAFAC-SVD)

In this work, we assume that the code ($\mathbf{C}$ and $\mathbf{G}$) matrices are known at the destination node. The first row ($\mathbf{S}_{\mathbf{1}.}$) of the symbol matrix is also assumed known and formed of ones, which means that the first symbol sent by each antenna of the source node is chosen equal to 1. Due to the knowledge of the matrix factor $\mathbf{C}$, there is no column permutation ambiguity for any solution ($\mathbf{H}^{(SD)}$, $\mathbf{S}$) of the PARAFAC model of the direct link.

Assuming that $\mathbf{C}$ is full-column rank and post-multiplying (6) by $(\mathbf{C}^T)^\dagger$ give $\mathbf{X} = \mathbf{Y}_{NM_D \times P}^{(SD)} (\mathbf{C}^T)^\dagger = \mathbf{H}^{(SD)} \diamond \mathbf{S}$. So, we can use SVD-based rank-1 approximations to estimate $\mathbf{S}$ and $\mathbf{H}^{(SD)}$ from their Khatri-Rao product, which leads to the following closed-form solution [28], [32], [33]

For $m_S = 1, \cdots, M_S$:

- Apply the *unvec(.)* operator to reshape the m_S^{th}-column vector of $\mathbf{X}$ into a matrix $\mathbf{A}(m_S) \in \mathbb{C}^{N \times M_D}$ such as:

$$\begin{aligned}\mathbf{A}(m_S) &= unvec(\mathbf{X}_{.m_S}) = unvec(\mathbf{H}_{.m_S}^{(SD)} \otimes \mathbf{S}_{.m_S}) \\ &= \mathbf{S}_{.m_S} \mathbf{H}_{.m_S}^{(SD)^T}.\end{aligned}$$

- Compute the SVD of $\mathbf{A}(m_S) = \mathbf{U}\mathbf{\Sigma}\mathbf{V}^H$, with the singular values ordered in a decreasing order on the diagonal of $\mathbf{\Sigma}$.

- Assuming that $s_{1,m_S} = 1$ for $m_S = 1, \cdots, M_S$, we deduce the following estimated values $\hat{\mathbf{S}}_{.m_S} = \mathbf{U}_{.1}/u_{1,1}$ and $\hat{\mathbf{H}}^{(SD)}_{.m_S} = \mathbf{V}^*_{.1} u_{1,1}\sigma_{1,1}$.

B. Link via relay: ALS-based receivers

The channel $(\mathbf{H}^{(SR)}, \mathbf{H}^{(RD)})$ and symbol $(\mathbf{S})$ matrices are jointly estimated by alternately minimizing the following conditional least squares (LS) criteria deduced from noisy versions of (10), (12) and (15) of the PARATUCK2 model:

$$J\left(\mathbf{h}^{(SR)}\right) = \left|\left|\widetilde{\mathbf{y}}^{(SRD)} - (\widehat{\mathbf{W}}_1)_{i-1}\mathbf{h}^{(SR)}\right|\right|_2^2 \quad (18)$$

$$\Rightarrow \ \widehat{\mathbf{h}}_i^{(SR)} = (\widehat{\mathbf{W}}_1)_{i-1}^{\dagger}\widetilde{\mathbf{y}}^{(SRD)} \quad (19)$$

$$J\left(\mathbf{H}^{(RD)}\right) = \left|\left|\widetilde{\mathbf{Y}}^{(SRD)}_{PN\times M_D} - (\widehat{\mathbf{W}}_2)_i\left(\mathbf{H}^{(RD)}\right)^T\right|\right|_F^2 \quad (20)$$

$$\Rightarrow \ \left(\widehat{\mathbf{H}}_i^{(RD)}\right)^T = (\widehat{\mathbf{W}}_2)_i^{\dagger}\widetilde{\mathbf{Y}}^{(SRD)}_{PN\times M_D} \quad (21)$$

$$J\left(\mathbf{s}_n\right) = \left|\left|\widetilde{\mathbf{y}}_n^{(SRD)} - (\widehat{\mathbf{W}}_3)_i\mathbf{s}_n\right|\right|_2^2 \quad (22)$$

$$\Rightarrow \ (\widehat{\mathbf{s}}_n)_i = (\widehat{\mathbf{W}}_3)_i^{\dagger}\widetilde{\mathbf{y}}_n^{(SRD)} \quad (23)$$

where i denotes the iteration number, $\widetilde{\mathbf{Y}}^{(SRD)}_{PN\times M_D}$ and $\widetilde{\mathbf{y}}^{(SRD)}$ are matricized and vectorized forms of the noisy tensor $\widetilde{\mathcal{Y}}^{(SRD)}$, and $(\widehat{\mathbf{W}}_j)_i$ is the value of $\mathbf{W}_j$, for $j = 1, 2, 3$, estimated at iteration i, by means of Eq. (24)-(28), deduced from (11), (13), (16), (14), and (17) in replacing the true system parameters by their previously estimated values:

$$(\widehat{\mathbf{W}}_1)_{i-1} = \left(\widehat{\mathbf{S}}_{i-1}^T \diamond \mathbf{G}^T\right)^T \diamond \left(\mathbf{C}\otimes\widehat{\mathbf{H}}_{i-1}^{(RD)}\right) \quad (24)$$

$$(\widehat{\mathbf{W}}_2)_i = (\mathbf{I}_N \otimes \mathbf{C})\widehat{\mathbf{F}}_i, \quad (25)$$

$$(\widehat{\mathbf{W}}_3)_i = \mathbf{C} \diamond (\widehat{\mathbf{Z}}_n^{(SRD)})_i. \quad (26)$$

with

$$\widehat{\mathbf{F}}_i = \begin{bmatrix} D_1\left(\widehat{\mathbf{S}}_{i-1}\right)\left(\widehat{\mathbf{H}}_i^{(SR)}\right)^T D_1(\mathbf{G}) \\ \vdots \\ D_N\left(\widehat{\mathbf{S}}_{i-1}\right)\left(\widehat{\mathbf{H}}_i^{(SR)}\right)^T D_N(\mathbf{G}) \end{bmatrix} \quad (27)$$

$$\left(\widehat{\mathbf{Z}}_n^{(SRD)}\right)_i = \widehat{\mathbf{H}}_i^{(RD)} D_n(\mathbf{G})\widehat{\mathbf{H}}_i^{(SR)}. \quad (28)$$

The symbols can also be estimated by combining (8) and (15) to form the following cost function

$$J(\mathbf{s}_n) = \left|\left|\widetilde{\mathbf{y}}_n^{(C)} - \begin{bmatrix} \mathbf{C}\diamond\widehat{\mathbf{H}}_{i-1}^{(SD)} \\ \mathbf{C}\diamond(\widehat{\mathbf{Z}}_n^{(SRD)})_i \end{bmatrix}\mathbf{s}_n\right|\right|_2^2$$

$$\Rightarrow \ (\hat{\mathbf{s}}_n)_i = \begin{bmatrix} \mathbf{C}\diamond\widehat{\mathbf{H}}_{i-1}^{(SD)} \\ \mathbf{C}\diamond(\widehat{\mathbf{Z}}_n^{(SRD)})_i \end{bmatrix}^{\dagger}\widetilde{\mathbf{y}}_n^{(C)}, \quad (29)$$

where

$$\mathbf{y}_n^{(C)} = \begin{bmatrix} \mathbf{y}_n^{(SD)} \\ \mathbf{y}_n^{(SRD)} \end{bmatrix} \in \mathbb{C}^{2M_D P\times 1}. \quad (30)$$

TABLE I
SEMI-BLIND RECEIVERS

	PARATUCK2-ALS	SPP-ALS	CPP-ALS
Step 1 Initialization ($i = 0$)	$\hat{\mathbf{S}}_0$ random	PARAFAC-SVD Section IV-A	
		$\hat{\mathbf{S}}_0 \leftarrow \hat{\mathbf{S}}_{SVD}$	$\hat{\mathbf{S}}_0 \leftarrow \hat{\mathbf{S}}_{SVD}$ $\hat{\mathbf{H}}_0^{(SD)} \leftarrow \hat{\mathbf{H}}_{SVD}^{(SD)}$
	$\hat{\mathbf{H}}_0^{(RD)}$ random		
Step 2 Iteration	$i \leftarrow i+1$		
2.1 Channel estimation	Calculation of $\hat{\mathbf{h}}_i^{(SR)}$ using Eq. (19) and (24) Calculation of $\hat{\mathbf{H}}_i^{(RD)}$ using Eq. (21), (25) and (27)		
2.2 Symbol estimation	Calculation of $(\hat{\mathbf{s}}_n)_i$ for $n = 1, \cdots, N$		
	Eq. (23), (26), and (28)		Eq. (29)-(30)
2.3 Refinement of $\hat{\mathbf{H}}^{(SD)}$			Eq. (31)
Step 3	Go to step 2 until convergence		

The estimate $\widehat{\mathbf{H}}_{i-1}^{(SD)}$ used in (29) is updated at each iteration by the following equation, deduced from Eq. (5)

$$\left(\widehat{\mathbf{H}}_i^{(SD)}\right)^T = \left(\widehat{\mathbf{S}}_i \diamond \mathbf{C}\right)^{\dagger}\widetilde{\mathbf{Y}}^{(SD)}_{PN\times M_D}. \quad (31)$$

In Table 1, we propose three ALS-based receivers. The first one, called PARATUCK2-ALS algorithm, uses only the PARATUCK2 model for estimating the channel ($\mathbf{H}^{(SR)}$ and $\mathbf{H}^{(RD)}$) and symbol ($\mathbf{S}$) matrices, with a random initialization ($\hat{\mathbf{S}}_0$, $\hat{\mathbf{H}}_0^{(RD)}$).

The two other ones, respectively called Sequential PARAFAC/PARATUCK2 (SPP) and Combined PARAFAC/PARATUCK2 (CPP) algorithms, use both the PARAFAC and the PARATUCK2 models. For the SPP receiver, the direct link is used for initializing $\widehat{\mathbf{S}}_0$ as the solution of the PARAFAC-SVD algorithm presented in subsection IV-A, and then the system parameters are estimated using Eq. (19), (21) and (23).

For the CPP receiver, the initial values $\widehat{\mathbf{S}}_0$ and $\widehat{\mathbf{H}}_0^{(SD)}$ are also calculated from the PARAFAC-SVD algorithm, and the symbol vector $\mathbf{s}_n$ is estimated using Eq. (29)-(31), i.e. by jointly exploiting the signals received from the direct link and the link via relay.

It is important to note that the three receivers differ only in the initialization (step 1) and the symbol estimation (steps 2.2 and 2.3).

C. Discussion

KRST coding at the source allows to jointly and semi-blindly estimate the channel and symbol matrices by processing the signals received at the destination node via the relay or/and the direct link, i.e. by exploiting the PARATUCK2 model or/and the PARAFAC model. As the direct link is generally characterized by a lower SNR than the relay-assisted link due to signal amplification by the relay, the transmitted symbols are better estimated using the SRD link, i.e. the tensor $\mathcal{Y}^{(SRD)}$ of received signals.

On the other hand, the performance of the PARATUCK2-ALS receiver greatly depends on initialization. Due to the absence of *a priori* information on channels, a random initialization is used, which generally implies a slow convergence.

A performance improvement can be obtained by initializing the PARATUCK2-ALS receiver with symbol initial values ($\widehat{\mathbf{S}}_0$) provided by the PARAFAC-SVD algorithm associated with the direct link. That is the idea behind the SPP and CPP receivers (see step 1 in Table 1).

Since each block of signals transmitted via the SD link is received right after the first hop of the protocol, and due to the fast computation of the PARAFAC-SVD method, this processing is likely finished before the end of the second hop, during which the relay forwards the amplified signals. Therefore, the use of the SD link does not increase the total estimation time, but on the contrary, the overall computational cost can be reduced using a better initialization for the PARATUCK2-ALS algorithm. From another point of view, combining the two models for estimating the symbols is equivalent to double the number of receive antennas at the destination node (see (29)-(30)), which implies an increase of space diversity and consequently a performance improvement. That is the idea exploited by the CPP receiver (see steps 2.2–2.3 in Table 1).

D. Uniqueness issue

For the PARATUCK2 model of the link via relay, we show in Appendix B that a simple design of $\mathbf{G}$ allows to ensure uniqueness of $\left(\mathbf{S}, \mathbf{H}^{(RD)}, \mathbf{H}^{(SR)}\right)$ up to column scaling ambiguities such that any alternative solution $\left(\bar{\mathbf{S}}, \bar{\mathbf{H}}^{(RD)}, \bar{\mathbf{H}}^{(SR)}\right)$ satisfies the following equations

$$\bar{\mathbf{S}} = \mathbf{S},$$
$$\bar{\mathbf{H}}^{(RD)}\boldsymbol{\Delta}^{(RD)} = \mathbf{H}^{(RD)}, \tag{32}$$
$$\left(\boldsymbol{\Delta}^{(RD)}\right)^{-1}\bar{\mathbf{H}}^{(SR)} = \mathbf{H}^{(SR)}, \tag{33}$$

where $\boldsymbol{\Delta}^{(RD)} \in \mathbb{C}^{M_R \times M_R}$ is a complex diagonal matrix.

This scaling ambiguity $\boldsymbol{\Delta}^{(RD)}$ can be eliminated using the knowledge of one row of $\mathbf{H}^{(RD)}$ or one column of $\mathbf{H}^{(SR)}$, as mentioned in [18], [30]. In practice, such a knowledge can be obtained by means of a simple supervised procedure which consists in sending a training sequence from the relay to destination and applying the standard LS algorithm to estimate the channel $\mathbf{H}^{(RD)}$ that can be used to calculate the scaling ambiguity matrix $\boldsymbol{\Delta}^{(RD)}$. When an individual channel estimation is not needed, it is important to notice that our receivers are robust to channel ambiguities due to the fact that symbol estimation by means of (23) or (29) only depends on the effective channel defined in (17), which is without scaling ambiguity since $\bar{\mathbf{H}}^{(RD)}D_n(\mathbf{G})\bar{\mathbf{H}}^{(SR)} = \mathbf{H}^{(RD)}D_n(\mathbf{G})\mathbf{H}^{(SR)}$.

E. Identifiability conditions

Necessary and sufficient conditions for system identifiability with the PARATUCK2-, SPP-, and CPP-ALS algorithms are directly linked to the full column-rank condition to be satisfied by the arguments of the pseudo-inverse operators that result from the minimization of the LS cost functions (18), (20) and (22). That leads to the following theorem.

Theorem 1 (*Sufficient conditions for identifiability of relay-assisted link*) Assuming that $\mathbf{H}^{(RD)}$ and $\mathbf{H}^{(SR)}$ have independent and identically distributed (i.i.d.) entries drawn from a continuous distribution (rich scattering assumption), joint identifiability of the channel ($\mathbf{H}^{(RD)}$, $\mathbf{H}^{(SR)}$) and symbol ($\mathbf{S}$) matrices in the LS sense is guaranteed if $\mathbf{S}$ and $\mathbf{G}$ do not contain zero element, and if the code $\mathbf{C}$ and the channel $\mathbf{H}^{(RD)}$ matrices are full column rank, and the channel matrix $\mathbf{H}^{(SR)}$ is full row rank, which implies the following inequalities for some design parameters

$$P \geq M_S \quad \text{and} \quad \mathit{Min}(M_S, M_D) \geq M_R. \tag{34}$$

Proof: From (10) , (12) and (15), we have $\mathbf{y}^{(SRD)} = \mathbf{W}_1\mathbf{h}^{(SR)}$, $\mathbf{Y}^{(SRD)}_{PN\times M_D} = \mathbf{W}_2\left(\mathbf{H}^{(RD)}\right)^T$ and $\mathbf{y}^{(SRD)}_n = \mathbf{W}_3\mathbf{s}_n$, where $\mathbf{W}_1$, $\mathbf{W}_2$ and $\mathbf{W}_3$ are defined in (11), (13), and (16), respectively. We deduce that the system identifiability in the LS sense requires that $\mathbf{W}_1$, $\mathbf{W}_2$ and $\mathbf{W}_3$ be full column rank.

Now, we determine under which conditions these matrices are full column rank.

Applying the lemma 1 in [34] which establishes that the Khatri-Rao product of $\mathbf{A} \in \mathbb{C}^{I\times R}$ and $\mathbf{B} \in \mathbb{C}^{J\times R}$ is full column rank if $k_{\mathbf{A}} + k_{\mathbf{B}} \geq R+1$, we can conclude that $\mathbf{W}_1$ defined in (11) is full column rank if

$$k_{(\mathbf{S}^T\diamond\mathbf{G}^T)^T} + k_{\mathbf{C}\otimes\mathbf{H}^{(RD)}} \geq M_R M_S + 1 \tag{35}$$

where $k_{\mathbf{A}}$ denotes the k-rank of $\mathbf{A}$ [35].

Assuming that $\mathbf{S}$ and $\mathbf{G}$ do not contain zero element ($k_{\mathbf{S}} \geq 1$ and $k_{\mathbf{G}} \geq 1$), we have $k_{(\mathbf{S}^T\diamond\mathbf{G}^T)^T} \geq 1$. Moreover, under the assumptions enounced in Theorem 1 ($\mathbf{C}$ and $\mathbf{H}^{(RD)}$ full column rank), we can conclude that the Kronecker product $\mathbf{C}\otimes\mathbf{H}^{(RD)}$ is full column rank, i.e. $k_{\mathbf{C}\otimes\mathbf{H}^{(RD)}} = M_R M_S$, and consequently (35) is satisfied, which implies that $\mathbf{W}_1$ is full column rank.

From (13), we can deduce that $\mathbf{W}_2$ is full column rank if $\mathbf{C}$ and $\mathbf{F}$ are also full column rank, which is the case of $\mathbf{C}$ by assumption. Considering the first row block of $\mathbf{F}$ in (14), it is easy to verify that the assumptions of Theorem 1 ensure that this block, and consequently $\mathbf{F}$, are full column rank. Finally, by applying again the Lemma 1 in [34], with $k_{\mathbf{C}} = M_S$ and $k_{\mathbf{Z}_n^{(SRD)}} \geq 1$, we deduce that $\mathbf{W}_3$ defined in (16)-(17) is full column rank. That concludes the proof of Theorem 1. ■

Remark 1: Theorem 1 has been proved by resorting to condition (35), which is sufficient but not necessary for identifying $\mathbf{h}^{(SR)}$. Indeed, as shown in our simulation results, identifiability of $\mathbf{h}^{(SR)}$ is even possible when $M_D < M_R$. Necessary conditions, based on the external dimensions of $\mathbf{W}_1$, $\mathbf{W}_2$ and $\mathbf{W}_3$, are respectively $M_D PN \geq M_R M_S$, $PN \geq M_R$ and $M_D P \geq M_S$, which are all satisfied when the conditions (34) of Theorem 1 are satisfied.

Remark 2: When the assumptions of Theorem 1 are satisfied, implying that $\mathbf{C}$ is full column rank, the PARAFAC-SVD receiver described in subsection IV-A can be applied for estimating $\mathbf{S}$ and $\mathbf{H}^{(SD)}$, i.e. initializing the SPP- and CPP-ALS receivers (see step 1 in Table I).

V. SIMULATIONS

In this section, the performance of the proposed receivers are evaluated by means of Monte Carlo simulations. Since our tensor-based receivers are concerned with symbol and channel estimation, we are interested in evaluating both the bit error rate (BER) performance and the channel NMSE given by

$$\text{NMSE} = \frac{1}{M}\left(\sum_{m=1}^{M}\frac{||\mathbf{H}_m^{(\mathit{eff})} - (\widehat{\mathbf{H}}_\infty^{(\mathit{eff})})_m||_F^2}{||\mathbf{H}_m^{(\mathit{eff})}||_F^2}\right), \tag{36}$$

where M = 2000 denotes the number of Monte Carlo runs, $\mathbf{H}_m^{(\mathit{eff})} = \mathbf{H}_m^{(RD)}\mathbf{H}_m^{(SR)}$ is the effective channel generated at the m^{th} run, and $(\widehat{\mathbf{H}}_\infty^{(\mathit{eff})})_m$ is calculated using estimates $(\hat{\mathbf{H}}_\infty^{(RD)})_m$ and $(\hat{\mathbf{H}}_\infty^{(SR)})_m$ obtained at convergence of the considered receiver algorithms.

The code matrix $\mathbf{C}$ is chosen as a truncated discrete Fourier transform (DFT) matrix with $c_{p,m_S} = exp\left(\frac{2j\pi(p-1)(m_S-1)}{M_S}\right)$ and $P \geq M_S$. Following the motivation of [27], this choice ensures that $\mathbf{C}$ has full column rank, which is a necessary condition for maximizing the diversity gain and a condition of Theorem 1 for identifiability. This structure is also flexible in the sense that rate/diversity can be controlled by truncation. The relay gain $\mathbf{G}$ is chosen as a Vandermonde matrix with random generators (see Eq. (53), in Appendix B). This design avoids permutation ambiguities in the estimation of $\mathbf{H}^{(SR)}$ and $\mathbf{H}^{(RD)}$, and it is a good choice from the identifiability viewpoint. It is worth noting that, though the code matrices ($\mathbf{C}$, $\mathbf{G}$) are fixed with a particular structure for joint channel/symbol estimation purpose, their design could be optimized once an estimate of the channel matrices is available at the source and/or relay nodes [11], [36]. A 4-PSK modulation with uniform distribution of symbols is used to generate the matrix $\mathbf{S} = \sqrt{E_S}\mathbf{S}_o$ at each run, where $\mathbf{S}_o$ is a matrix composed of unit energy symbols, and E_S is the symbol energy. In some simulations, the BER and the channel NMSE are evaluated as functions of E_S.

Channel matrices $\mathbf{H}^{(RD)}$, $\mathbf{H}^{(SR)}$ and $\mathbf{H}^{(SD)}$ have i.i.d. entries drawn from complex Gaussian distributions with zero mean and variances $1/M_R$, $1/M_S$, and $\frac{10^{-\alpha/10}}{M_S}$, respectively, where α is a tuning parameter allowing to set the energy of the SD link relatively to that of the SRD link (see Eq. (38)). The entries of the noise tensors $\mathcal{V}^{(R)}$ and $\mathcal{V}^{(D)}$ have the same distribution, but with a unit variance. From the above assumptions we deduce $E\left\{\mathbf{H}^{(SR)}\left(\mathbf{H}^{(SR)}\right)^H\right\} = E\left\{D_n(\mathbf{G})D_n^H(\mathbf{G})\right\} = \mathbf{I}_{M_R}$, $E\left\{\mathbf{H}^{(RD)}\left(\mathbf{H}^{(RD)}\right)^H\right\} = \mathbf{I}_{M_D}$, and $E\left\{\mathbf{H}^{(SD)}\left(\mathbf{H}^{(SD)}\right)^H\right\} = 10^{-\alpha/10}\mathbf{I}_{M_D}$. Both signal-to-noise ratios (SNRs) of the SRD and SD links are proportional to E_S since the noise-free signals are proportional to E_S. The ratio between the energies of the SRD link at the n^{th} time-block (deduced from (17)) and the direct link is given by

$$\frac{tr\left[\mathbf{R}^{(SRD)}\right]}{tr\left[\mathbf{R}^{(SD)}\right]} = \frac{E\left\{||\mathbf{Z}_n^{(SRD)}||_F^2\right\}}{E\left\{||\mathbf{H}^{(SD)}||_F^2\right\}} = \frac{tr\left[E\left\{\mathbf{H}^{(RD)}\left(\mathbf{H}^{(RD)}\right)^H\right\}\right]}{tr\left[E\left\{\mathbf{H}^{(SD)}\left(\mathbf{H}^{(SD)}\right)^H\right\}\right]} = 10^{\alpha/10}, \tag{37}$$

where $tr[.]$ is the trace operator. From (37), we deduce that α in dB represents the difference between the energies of the SRD and SD channels, i.e.

$$\alpha_{(dB)} = 10\log\left(tr\left[\mathbf{R}^{(SRD)}\right]\right) - 10\log\left(tr\left[\mathbf{R}^{(SD)}\right]\right). \tag{38}$$

The simulation results show that the energy of the direct link (set by α) has a relevant impact on the performance of the SPP-ALS and CPP-ALS receivers.

The maximum number of ALS iterations for the proposed algorithms is set to 1000, and the convergence is declared at the i^{th} iteration when $\xi_i - \xi_{i-1} \leq 10^{-6}$, where ξ_i is the reconstruction error at iteration i, defined as

$$\xi_i = \frac{\left|\left|\tilde{\mathbf{Y}}_{PN\times M_D}^{(SRD)} - (\mathbf{I}_N \otimes \mathbf{C})\widehat{\mathbf{F}}_i\left(\widehat{\mathbf{H}}_i^{(RD)}\right)^T\right|\right|_F^2}{\left|\left|\tilde{\mathbf{Y}}_{PN\times M_D}^{(SRD)}\right|\right|_F^2}. \tag{39}$$

The transmission rate for the three proposed semi-blind receivers (PARATUCK2, SPP and CPP) is equal to $r = (N-1)M_S/(2PN)$ data symbols per symbol period, since $(N-1)M_S$ information symbols are transmitted during the two transmission phases of NP symbol periods each.

For each figure, the parameters common to all curves are indicated on the top of itself, while the parameters characterizing each curve are given in the legend.

A. Pilot-based channel estimators

We compare our semi-blind receivers with two supervised receivers for estimating the channels $\mathbf{H}^{(SR)}$ and $\mathbf{H}^{(RD)}$ without coding at the source.

1) BALS channel estimator [18]: In [18], the noiseless signals received via the SRD link, during the n^{th} time-block, are given by $\mathbf{Y}_{..n}^{(SRD)} = \mathbf{H}^{(RD)}D_n(\mathbf{G})\mathbf{H}^{(SR)}\bar{\mathbf{S}} \in \mathbb{C}^{M_D\times L}$, where the pilot symbol matrix $\bar{\mathbf{S}} \in \mathbb{C}^{M_S\times L}$ is chosen as a DFT matrix, L being the length of the training sequence, with $L \geq M_S$. The filtered signals $\mathbf{X}_{..n}^{(SRD)} = \mathbf{Y}_{..n}^{(SRD)}\bar{\mathbf{S}}^H = \mathbf{H}^{(RD)}D_n(\mathbf{G})\mathbf{H}^{(SR)}$ satisfy a PARAFAC model whose matrix factors $\mathbf{H}^{(SR)}$ and $\mathbf{H}^{(RD)}$ can be estimated using a bilinear ALS (BALS) algorithm based on the following equations

$$\widehat{\mathbf{H}}^{(SR)} = \left[\mathbf{G}\diamond\widehat{\mathbf{H}}^{(RD)}\right]^\dagger\tilde{\mathbf{X}}_{M_DN\times M_S}, \tag{40}$$

$$\left(\widehat{\mathbf{H}}^{(RD)}\right)^T = \left[(\widehat{\mathbf{H}}^{(SR)})^T\diamond\mathbf{G}\right]^\dagger\tilde{\mathbf{X}}_{NM_S\times M_D}, \tag{41}$$

2) LS-SVD channel estimator [28]: In [28], the same PARAFAC model as in [18] is used but the following unfolded form is exploited

$$\mathbf{X}_{M_D M_S \times N} = \left(\left(\mathbf{H}^{(SR)} \right)^T \diamond \mathbf{H}^{(RD)} \right) \mathbf{G}^T.$$

Assuming that $\mathbf{G}$ is full column rank which implies $N \geq M_R$, we have

$$\mathbf{X}_{M_D M_S \times N} (\mathbf{G}^T)^\dagger = \left(\left(\mathbf{H}^{(SR)} \right)^T \diamond \mathbf{H}^{(RD)} \right),$$

and the channels can be estimated using a closed-form (SVD-based) solution, like the one presented in subsection IV-A.

The BALS and LS-SVD receivers exploit the same received data with an iterative (i.e. BALS) and a closed-form (i.e. LS-SVD) method, respectively. Under the assumptions made in Theorem 1, from lemma 1 in [34] we can conclude that both Khatri-Rao products in (40) and (41) are full column-rank matrices, and therefore both channels can be estimated using the BALS estimator.

Note that both BALS and LS-SVD algorithms are only dedicated to channel estimation, and therefore the transmission rate of any system applying these methods depends on the transmission-reception protocol.

For both estimators, the BER results are obtained with a zero forcing (ZF) receiver that estimates M_S symbols during N_T time-blocks. The transmission of each symbol vector $\mathbf{s}_n \in \mathbb{C}^{M_S \times 1}$ is repeated during N_T time-blocks using N_T different AF gains, so that the received signal vector at the input of the ZF receiver is given by

$$\begin{aligned} \tilde{\mathbf{y}}_n^{(SRD)} &= \begin{bmatrix} \mathbf{H}^{(RD)} D_1(\mathbf{G}) \mathbf{H}^{(SR)} \\ \vdots \\ \mathbf{H}^{(RD)} D_{N_T}(\mathbf{G}) \mathbf{H}^{(SR)} \end{bmatrix} \mathbf{s}_n + \mathbf{v}_n^{(SRD)} \\ &= \mathbf{Z} \mathbf{s}_n + \mathbf{v}_n^{(SRD)} \in \mathbb{C}^{M_D N_T \times 1}, \end{aligned} \quad (42)$$

where $\mathbf{H}^{(SR)}$ and $\mathbf{H}^{(RD)}$ are estimated using (40)-(41) (see [18] for further details). The output of the ZF receiver is then given by

$$\widehat{\mathbf{s}}_n = \widehat{\mathbf{Z}}^\dagger \tilde{\mathbf{y}}_n^{(SRD)}.$$

where $\widehat{\mathbf{Z}}$ is calculated using the estimate values of $\mathbf{H}^{(SR)}$ and $\mathbf{H}^{(RD)}$. This ZF receiver exploits time diversity due to coding across N_T time-blocks at the relay. This is particularly useful when the number of receive antennas is smaller than the number of transmit antennas. By examining (15) and (42), we can see that $M_D P$-length and $M_D N_T$-length data blocks are used by the SPP receiver and ZF receiver, respectively, for estimating $\mathbf{s}_n$. For the CPP receiver, a $2M_D P$-length data block is used as shown in (30). Note that N_T and N do not need to be equal, as these design parameters are associated with two independent procedures (i.e. separate channel and symbol estimation) when using the ZF receiver.

B. SPP receiver: Initialization obtained from the SD link

The aim of these simulations is to highlight the benefits of exploiting the PARAFAC modeling of the SD link to initialize $\hat{\mathbf{S}}_0$ in the SPP-ALS receiver, comparatively with the baseline PARATUCK2-ALS receiver which uses a random initialization. In Fig. 2, the NMSE of the reconstruction error (39) is plotted versus the number of ALS iterations required for convergence, for three different values of α. We can see that when α is increased (i.e. the energy of the SD link is decreased) the SPP receiver converges more slowly. Indeed, due to the increase of α, the symbol estimates obtained via the SD link by the PARAFAC-SVD algorithm become less accurate, and then the initialization $\hat{\mathbf{S}}_0$ (step 1 in Table 1) becomes worse.

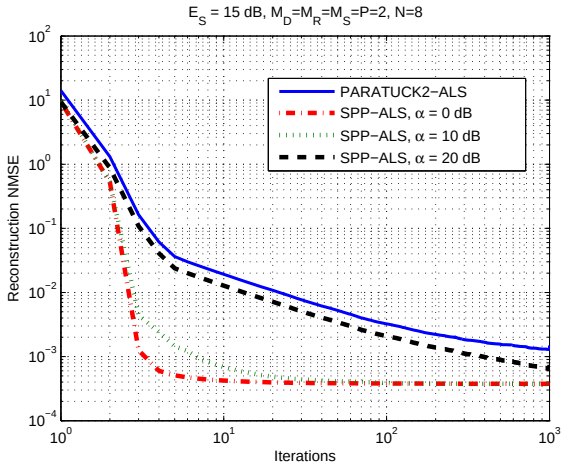

Fig. 2. NMSE *versus* iterations.

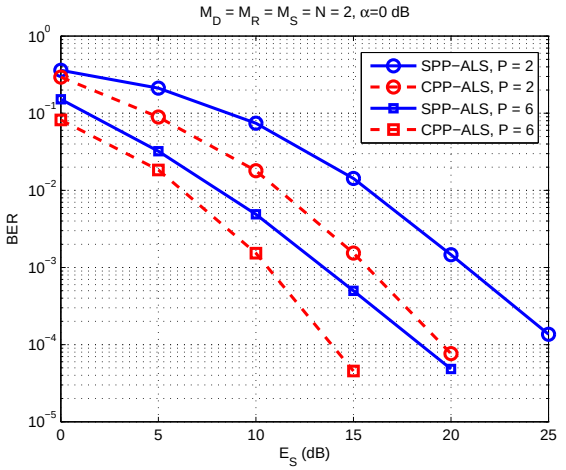

Fig. 3. BER *versus* E_S. Impact of P

C. Impact of P and M_D

Fig. 3 and 4 illustrate, respectively, the impact of the choice of P and M_D on the performance of the SPP- and CPP- ALS receivers. Fig. 3 depicts the BER curves for two values of P. We can see that, by increasing P, the performance of both receivers is clearly improved at the cost of a reduction of the transmission rate. The almost parallel shifts of the BER curves for both receivers corroborate the coding gain obtained by increasing P. Fig. 4 shows the impact of the number M_D of antennas at the destination. The slopes of the BER curves

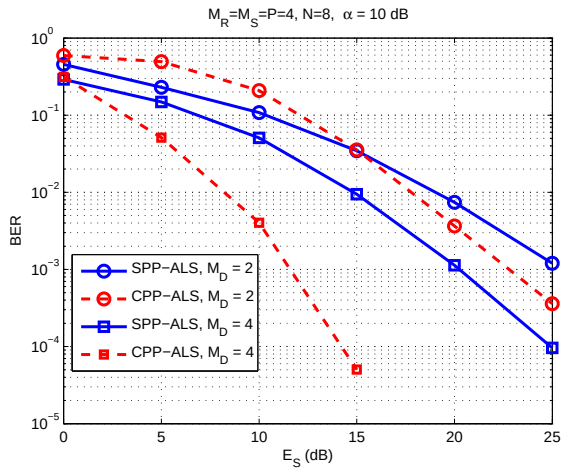

Fig. 4. BER *versus* E_S. Impact of M_D

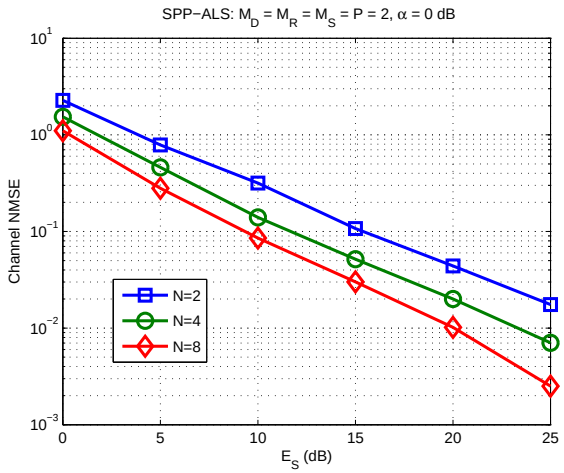

Fig. 5. NMSE *versus* E_S. Impact of N

indicate that the proposed receivers satisfactorily benefit from an additional spatial diversity when more antennas are used at the destination node. The performance improvement of CPP over SPP is due to an increase of space diversity with the CPP receiver, resulting from the combined use of the SD and SRD links for symbol estimation (cf. Eq. (29)). These results corroborate the more efficient use of cooperative diversity achieved by the CPP receiver.

D. Impact of N

Now a performance analysis is done in terms of the number N of time-blocks. Since the equations (23) and (29), used to estimate the symbols respectively by SPP-ALS and CPP-ALS receivers, take into account only a block at a time, the impact of changing N is mainly seen on the channel estimation. Fig. 5 shows the channel NMSE obtained with the SPP-ALS receiver for $N = \{2, 4, 8\}$. From this figure, we can conclude that increasing N provides a better channel estimation, since the estimation of the channels $\mathbf{H}^{(RD)}$ and $\mathbf{H}^{(SR)}$ using (19) and (21), and therefore of the effective channel NMSE calculated by (36), is depending on N. However, such an improvement of channel estimation is at the cost of a higher computational complexity, due to the increase of the dimensions of the matrices $\mathbf{W}_1$ and $\mathbf{W}_2$ to be pseudo-inverted.

E. Comparison with pilot-assisted receivers

In the following, we compare the channel NMSE and BER performances of SPP and CPP with those provided by the two competing pilot-assisted estimators (i.e. BALS [18] and LS-SVD [28]). For a fair comparison, the transmission rate and the number of transmitted symbols are fixed with the same values for all receivers. For each Monte Carlo run, the BER is calculated from a total of $(N-1)M_S$ symbols. For the BALS+ZF and LS-SVD+ZF receivers, N_T is chosen to satisfy the condition of existence for these ZF receivers (i.e. $\mathbf{Z}$ full column-rank in (42)).

The channel NMSE and the BER are plotted in Figs. 6 and 7, respectively. In Fig. 6, we can see that the pilot-assisted receivers present the best channel estimation performance, with

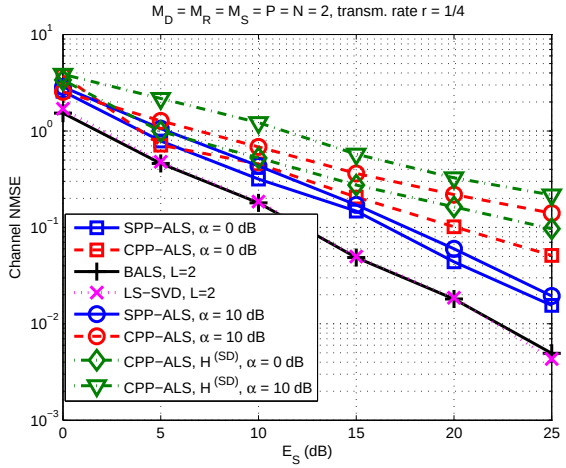

Fig. 6. NMSE *versus* E_S.

an indistinguishable difference between them. Such similarity between BALS and LS-SVD was expected, since they exploit the same data tensor in two different ways. The performance gain obtained with these receivers is due to the use of pilot symbols, which is not the case with the proposed SPP and CPP receivers. Moreover, we can see that the energy level of the direct link clearly impacts the channel estimation performance of our receivers. While the SPP receiver benefits from the SD link only to initialize the PARATUCK2-ALS algorithm (cf. Table 2, step 1), the CPP receiver also uses updated estimates $\hat{\mathbf{H}}^{(SD)}$ to (re-)estimate the symbols at each iteration (cf. Table 1, step 2.2). Therefore, reducing the energy of the direct link (i.e. increasing α) slightly degrades the performance of the SPP receiver, while the performance degradation is more sensitive with the CPP receiver.

The impact of α is also observed in the BER curves (Fig. 7). For the SPP receiver, the BER curves follow the tendency observed in the NMSE curves (Fig. 6). Concerning the CPP receiver, we can see it is more sensitive to the quality of the SD link. For $\alpha = 0$ dB, the estimate of $\mathbf{H}^{(SD)}$ is more accurate. Consequently, the use of the SD link in the CPP-ALS algorithm benefits the overall receiver performance. On

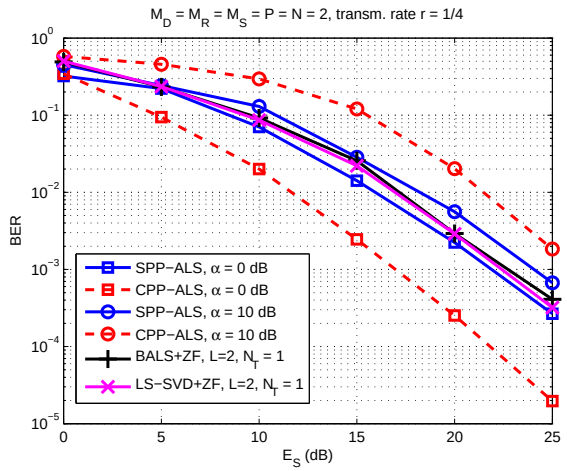

Fig. 7. BER *versus* E_S.

the other hand, when $\alpha = 10$ dB, a poorer quality of the SD link leads to worse estimates of $\mathbf{H}^{(SD)}$ and $\mathbf{s}_n$.

In summary, the competing and the proposed receivers exploit different tensor models and involve different tasks. The two pilot-assisted channel estimation methods (LS-SVD and BALS) are less computationally demanding than the proposed semi-blind SPP and CPP receivers. In particular, the closed-form LS-SVD method has the smallest computational cost among the considered methods, followed by the BALS estimator. Nevertheless, our semi-blind receivers allow a joint channel and symbol estimation while benefiting from the code diversity introduced by the simplified Khatri-Rao coding at the source node. It was also observed that the CPP receiver is more sensitive to the use of the SD link. For a weak direct link, the performance degradation of the CPP receiver is more pronounced than that of the SPP receiver. On the other hand, a strong direct link may not bring significant performance gains for the SPP receiver, but definitely improves symbol estimation performance of the CPP receiver.

VI. Conclusion and Perspectives

We have proposed three new tensor-based receivers for two-hop cooperative MIMO relay systems exploiting spatial, time and code diversities. The proposed receivers arise from the use of a simplified KRST coding at the source node combined with an AF coding scheme at the relay node, leading to third-order received data tensors at the destination. The combination of PARAFAC and PARATUCK2 models of the direct link and the relay-assisted link, respectively, induces the formulation of two hybrid PARAFAC/PARATUCK2 receivers, namely the sequential PARAFAC/PARATUCK2 (SPP) and the combined PARAFAC/PARATUCK2 (CPP) receivers. These receivers avoid the use of training sequences, alleviate the computational complexity at the relay node and take advantage of the availability of the SD link in a two-hop relaying scenario. Along the development of these receivers, the identifiability issue has been discussed, and conditions for joint symbol and channel recovery at the destination have been derived. Some perspectives of this work include the development of new tensor-based receivers for MIMO relay systems operating with different coding structures at the source and/or relays, as well as under different relaying strategies (such as bidirectional and/or full-duplex relaying).

Appendix

A. Derivation of $\mathbf{y}^{(SRD)}$ and $\mathbf{Y}^{(SRD)}_{PN\times M_D}$

Applying the *vec*(.) operator to (9), and using twice the property (2) give

$$\begin{aligned}\mathbf{y}_n^{(SRD)} &= (\mathbf{C}\otimes\mathbf{H}^{(RD)})\text{vec}(D_n(\mathbf{G})\mathbf{H}^{(SR)}D_n(\mathbf{S}))\\ &= (\mathbf{C}\otimes\mathbf{H}^{(RD)})(D_n(\mathbf{S})\otimes D_n(\mathbf{G}))\mathbf{h}^{(SR)}.\end{aligned} \quad (43)$$

Collecting the data received during N symbol periods of P time-blocks, we obtain the following vectorized form of the received signal tensor $\mathcal{Y}^{(SRD)}$

$$\mathbf{y}^{(SRD)} = \begin{bmatrix}\mathbf{y}_1^{(SRD)}\\ \vdots \\ \mathbf{y}_N^{(SRD)}\end{bmatrix} \in \mathbb{C}^{M_DPN\times 1}. \quad (44)$$

Since $D_n(\mathbf{S})\otimes D_n(\mathbf{G}) = D_n\left(\left(\mathbf{S}^T\diamond\mathbf{G}^T\right)^T\right) \in \mathbb{C}^{M_RM_S\times M_RM_S}$, replacing (43) into (44) leads to

$$\mathbf{y}^{(SRD)} = \begin{bmatrix}\left(\mathbf{C}\otimes\mathbf{H}^{(RD)}\right)D_1\left(\left(\mathbf{S}^T\diamond\mathbf{G}^T\right)^T\right)\\ \vdots \\ \left(\mathbf{C}\otimes\mathbf{H}^{(RD)}\right)D_N\left(\left(\mathbf{S}^T\diamond\mathbf{G}^T\right)^T\right)\end{bmatrix}\mathbf{h}^{(SR)}. \quad (45)$$

Using the definition (1) of the Khatri-Rao product, we can rewrite (45) as (10).

By definition, the unfolded form $\mathbf{Y}^{(SRD)}_{PN\times M_D}$ can be developed as

$$\mathbf{Y}^{(SRD)}_{PN\times M_D} = \begin{bmatrix}\left(\mathbf{Y}^{(SRD)}_{..1}\right)^T\\ \vdots \\ \left(\mathbf{Y}^{(SRD)}_{..N}\right)^T\end{bmatrix},$$

Using the definition (9) of $\mathbf{Y}^{(SRD)}_{..n}$ gives

$$\mathbf{Y}^{(SRD)}_{PN\times M_D} = \begin{bmatrix}\mathbf{C}D_1(\mathbf{S})\left(\mathbf{H}^{(SR)}\right)^TD_1(\mathbf{G})\\ \vdots \\ \mathbf{C}D_N(\mathbf{S})\left(\mathbf{H}^{(SR)}\right)^TD_N(\mathbf{G})\end{bmatrix}\left(\mathbf{H}^{(RD)}\right)^T.$$

B. Design of the AF matrix $\mathbf{G}$

In [31], uniqueness properties of the PARATUCK2 decomposition were established under the following assumptions: i) Full rank matrices; ii) $\mathbf{H}^{(SR)}$ with entries different from zero; iii) Matrices $\mathbf{G}$ and $\mathbf{S}$ with the same number of columns ($M_R = M_S$). Uniqueness is then ensured up to column scaling and permutation ambiguities defined by means of the following equations

$$\bar{\mathbf{H}}^{(RD)}\left(\mathbf{P}\mathbf{\Delta}^{(RD)}\right) = \mathbf{H}^{(RD)}, \quad (46)$$

$$\bar{\mathbf{C}}\left(\mathbf{Q}\mathbf{\Delta}^{(C)}\right) = \mathbf{C} \quad (47)$$

$$\mathbf{\Delta}^{(G)}\left(\mathbf{\Delta}^{(RD)}\right)^{-1}\mathbf{P}^T\bar{\mathbf{H}}^{(SR)}\mathbf{Q}\left(\mathbf{\Delta}^{(C)}\right)^{-1}\mathbf{\Delta}^{(S)}=\mathbf{H}^{(SR)}, \tag{48}$$

where $\mathbf{P}\in\mathbb{R}^{M_R\times M_R}$ and $\mathbf{Q}\in\mathbb{R}^{M_S\times M_S}$ are permutation matrices, and ($\mathbf{\Delta}^{(C)}$, $\mathbf{\Delta}^{(G)}$, $\mathbf{\Delta}^{(S)}$, $\mathbf{\Delta}^{(RD)}$) are diagonal matrices, and for any n

$$\left(z_n^{-1}\mathbf{P}^T\right)D_n\left(\bar{\mathbf{G}}\right)\left(\mathbf{P}\left(\mathbf{\Delta}^{(G)}\right)^{-1}\right)=D_n(\mathbf{G}), \tag{49}$$

$$\left(z_n\mathbf{Q}^T\right)D_n\left(\bar{\mathbf{S}}\right)\left(\mathbf{Q}\left(\mathbf{\Delta}^{(S)}\right)^{-1}\right)=D_n(\mathbf{S}), \tag{50}$$

In this work, we assume that $\mathbf{C}$ and $\mathbf{G}$ are known at the destination. From (47), we deduce that $\mathbf{Q}=\mathbf{\Delta}^{(C)}=\mathbf{I}_{M_S}$.

Furthermore, if the first row of $\mathbf{S}$ is also known at the destination, we deduce from (50) that $\mathbf{\Delta}^{(S)}=z_1\mathbf{I}_{M_S}$.

Assuming that $\mathbf{P}=\mathbf{I}_{M_R}$, knowledge of $\mathbf{G}$ allows to deduce from Eq. (49) that $\mathbf{\Delta}^{(G)}=z_n^{-1}\mathbf{I}_{M_R}$ and consequently $z_n=z$ for all $n=1,...,N$. Equations (46) and (48) are then simplified as

$$\bar{\mathbf{H}}^{(RD)}\mathbf{\Delta}^{(RD)}=\mathbf{H}^{(RD)}$$
$$\left(\mathbf{\Delta}^{(RD)}\right)^{-1}\bar{\mathbf{H}}^{(SR)}=\mathbf{H}^{(SR)},$$

which corresponds to (32) and (33), respectively.

Now, we show how to choose the gain matrix $\mathbf{G}$ so that the permutation matrix $\mathbf{P}$ be equal to the identity matrix. Eq. (49) can be rewritten in scalar form, for $i=1,\cdots,M_R$, as

$$\left(z\delta_i^{(G)}\right)^{-1}\sum_{m_R=1}^{M_R}p_{m_R,i}^2g_{n,m_R}=g_{n,i} \tag{51}$$

where $p_{m_R,i}$ is the element (m_R,i) of $\mathbf{P}$, and $\delta_i^{(G)}$ is the i^{th} diagonal element of $\mathbf{\Delta}^{(G)}$.

Let us consider a permutation of two columns (i,j) of $\mathbf{G}$ such that $p_{j,i}=1$ with $i\neq j$. Application of this permutation to two rows n_1 and n_2 in (51) gives

$$\left(\delta_i^{(G)}\right)^{-1}=z\frac{g_{n_1,i}}{g_{n_1,j}}=z\frac{g_{n_2,i}}{g_{n_2,j}},$$

leading to $det(\mathbf{G}[n_1,n_2;i,j])=0$, where $\mathbf{G}[n_1,n_2;i,j]=\begin{bmatrix}g_{n_1,i} & g_{n_1,j}\\ g_{n_2,i} & g_{n_2,j}\end{bmatrix}$. A sufficient condition to avoid such a permutation is

$$det(\mathbf{G}[n_1,n_2;i,j])\neq 0. \tag{52}$$

Therefore, column permutations are avoided in $\mathbf{G}$ if the condition (52) is satisfied for any pair of rows (n_1,n_2) and all pairs of columns (i,j), which leads to the following general condition

$$det(\mathbf{G}[n_1,n_2;i,j])\neq 0\ \ \forall i\ \text{ and }\ j=1,...,M_R,\ \ i\neq j.$$

In this work we use a Vandermonde matrix for $\mathbf{G}$

$$\mathbf{G}=\begin{bmatrix}1 & 1 & \cdots & 1\\ e^{j\phi_1} & e^{j\phi_2} & \dots & e^{j\phi_{M_R}}\\ e^{j2\phi_1} & e^{j2\phi_2} & \dots & e^{j2\phi_{M_R}}\\ \vdots & \vdots & \ddots & \vdots\\ e^{j(N-1)\phi_1} & e^{j(N-1)\phi_2} & \dots & e^{j(N-1)\phi_{M_R}}\end{bmatrix}, \tag{53}$$

with random generators ϕ_{m_R}, $m_R=1,\cdots,M_R$, representing phase shifts introduced by the relay antennas. In the Monte Carlo simulations, these generators are drawn from a continuous uniform distribution between 0 and 2π.

Applying the condition (52) to the first two rows of $\mathbf{G}$ defined in (53), gives $\phi_j\neq\phi_i+2m\pi$ for $i\neq j$. As the phase shifts are randomly drawn, this condition is satisfied with a probability one.

REFERENCES

[1] A. Sendonaris, E. Erkip, and B. Aazhang, "User cooperation diversity - part I: system description," *IEEE Transactions on Communications*, vol. 51, no. 11, pp. 1927–1938, Nov. 2003.

[2] ——, "User cooperation diversity - part II: implementation aspects and performance analysis," *IEEE Transactions on Communications*, vol. 51, no. 11, pp. 1939–1948, Nov. 2003.

[3] J. N. Laneman, D. N. C. Tse, and G. W. Wornell, "Cooperative diversity in wireless networks: efficient protocols and outage behavior," *IEEE Transactions on Information Theory*, vol. 50, no. 12, pp. 3062–3080, Dec. 2004.

[4] R. Pabst, B. Walke, D. Schultz, P. Herhold, H. Yanikomeroglu, S. Mukherjee, H. Viswanathan, M. Lott, W. Zirwas, M. Dohler, H. Aghvami, D. Falconer, and G. Fettweis, "Relay-based deployment concepts for wireless and mobile broadband radio," *IEEE Communications Magazine*, vol. 42, no. 9, pp. 80–89, Sep. 2004.

[5] L. Cao, J. Zhang, and N. Kanno, "Multi-user cooperative communications with relay-coding for uplink IMT-advanced 4G systems," in *Proc. IEEE GLOBECOM'09*, Honolulu, HI, Dec. 2009, pp. 1–6.

[6] K. Liu, A. Sadek, W. Su, and A. Kwasinski, *Cooperative communications and networking*. Cambridge University Press, 2008.

[7] M. Dohler and Y. Li, *Cooperative communications: hardware, channel and PHY*. John Wiley & Sons, 2010.

[8] A. Nosratinia, T. E. Hunter, and A. Hedayat, "Cooperative communication in wireless networks," *IEEE Communications Magazine*, vol. 42, no. 10, pp. 74–80, Oct. 2004.

[9] P. Kumar and S. Prakriy, *Bidirectional Cooperative Relaying*. InTech, Apr. 2010.

[10] T. Unger and A. Klein, "Duplex schemes in multiple antenna two-hop relaying," *Elsevier Journal on Advances in Signal Processing*, vol. 2008, no. 92, pp. 1–18, Jan. 2008.

[11] M. Biguesh and A. Gershman, "Training-based MIMO channel estimation: a study of estimator tradeoffs and optimal training signals," *IEEE Transactions on Signal Processing*, vol. 54, no. 3, pp. 884–893, 2006.

[12] M. Shariat, M. Biguesh, and S. Gazor, "Relay design for SNR maximization in MIMO communication systems," in *2010 5th International Symposium on Telecommunications (IST)*, Tehran, Iran, 2010, pp. 313–317.

[13] Y. Rong, X. Tang, and Y. Hua, "A unified framework for optimizing linear nonregenerative multicarrier MIMO relay communication systems," *IEEE Transactions on Signal Processing*, vol. 57, no. 12, pp. 4837–4851, Dec. 2009.

[14] Y. Rong, "Optimal joint source and relay beamforming for MIMO relays with direct link," *IEEE Communications Letters*, vol. 14, no. 5, pp. 390–392, May 2010.

[15] F. Roemer and M. Haardt, "Tensor-based channel estimation (TENCE) for two-way relaying with multiple antennas and spatial reuse," in *IEEE International Conference on Acoustics, Speech and Signal Processing (ICASSP)*, Taipei, Taiwan, Apr. 2009, pp. 3641–3644.

[16] ——, "Tensor-based channel estimation and iterative refinements for two-way relaying with multiple antennas and spatial reuse," *IEEE Transactions on Signal Processing*, vol. 58, no. 11, pp. 5720–5735, Nov. 2010.

[17] C. A. R. Fernandes, A. L. F. de Almeida, and D. B. Costa, "Unified tensor modeling for blind receivers in multiuser uplink cooperative systems," *IEEE Signal Processing Letters*, vol. 19, no. 5, pp. 247 –250, May 2012.

[18] Y. Rong, M. Khandaker, and Y. Xiang, "Channel estimation of dual-hop MIMO relay system via parallel factor analysis," *IEEE Transactions on Wireless Communications*, vol. 11, no. 6, pp. 2224 –2233, Jun. 2012.

[19] R. A. Harshman, "Foundations of the PARAFAC procedure: Models and conditions for an "explanatory" multimodal factor analysis," *UCLA Working Papers in Phonetics*, vol. 16, pp. 1–84, Dec. 1970.

[20] J. D. Carroll and J.-J. Chang, "Analysis of individual differences in multidimensional scaling via an N-way generalization of "Eckart-Young" decomposition," *Psychometrika*, vol. 35, no. 3, pp. 283–319, Sep. 1970.
[21] N. D. Sidiropoulos, G. B. Giannakis, and R. Bro, "Blind PARAFAC receivers for DS-CDMA systems," *IEEE Transactions on Signal Processing*, vol. 48, no. 3, pp. 810–823, Mar. 2000.
[22] A. L. F. de Almeida, G. Favier, and J. C. M. Mota, "A constrained factor decomposition with application to MIMO antenna systems," *IEEE Transactions on Signal Processing*, vol. 56, pp. 2429–2442, Jun. 2008.
[23] ——, "Space-time spreading-multiplexing for MIMO wireless communications systems using the PARATUCK-2 tensor model," *Elsevier Signal Processing*, vol. 89, no. 11, pp. 2103–2116, Nov. 2009.
[24] G. Favier, M. N. da Costa, A. L. F. de Almeida, and J. M. Romano, "Tensor space-time (TST) coding for MIMO wireless communication systems," *Elsevier Signal Processing*, vol. 92, no. 4, pp. 1079–1092, Apr. 2012.
[25] A. L. F. de Almeida, G. Favier, and L. Ximenes, "Space-time-frequency (STF) MIMO communication systems with blind receiver based on a generalized PARATUCK2 model," *IEEE Transactions on Signal Processing*, vol. 61, no. 8, pp. 1895–1909, April 2013.
[26] T. Kong and Y. Hua, "Optimal channel estimation and training design for MIMO relays," in *IEEE Conference on Signals, Systems and Computers (ASILOMAR)*, Pacific Grove, CA, USA, Nov. 2010, pp. 663–667.
[27] N. D. Sidiropoulos and R. S. Budampati, "Khatri-Rao space-time codes," *IEEE Transactions on Signal Processing*, vol. 50, no. 10, pp. 2396–2407, Oct. 2002.
[28] P. Lioliou and M. Viberg, "Least-squares based channel estimation for MIMO relays," in *2008 International ITG Workshop on Smart Antennas (WSA)*, Darmstadt, Germany, 2008, pp. 90–95.
[29] R. A. Harshman and M. E. Lundy, "The PARAFAC model for three-way factor analysis and multidimensional scaling," *Research methods for multimode data analysis, H. G. Law, C.W. Snyder Jr., J. Hattie, and R. P. McDonald (Eds.)*, vol. 16, pp. 122–215, 1984.
[30] P. Lioliou, D. Svensson, and M. Viberg, "Channel tracking for AF MIMO relaying systems," in *IEEE 76th Vehicular Technology Conference (VTC2012-Fall)*, Québec city, Canada, Sept 2012.
[31] R. A. Harshman and M. E. Lundy, "Uniqueness proof for a family of models sharing features of Tucker′s three-mode factor analysis and PARAFAC/CANDECOMP," in *Psychometrika*, vol. 61, 1996, pp. 133–154.
[32] C. Van Loan and N. Pitsianis, "Approximation with Kronecker products," in *Linear Algebra for Large Scale and Real Time Applications*. Kluwer Publications, 1993, pp. 293–314.
[33] A. Y. Kibangou and G. Favier, "Noniterative solution for PARAFAC with a Toeplitz factor," in *7th European Signal Processing Conference (EUSIPCO-2009)*, Glasgow, Scotland, Aug 2009.
[34] N. D. Sidiropoulos, R. Bro, and G. B. Giannakis, "Parallel factor analysis in sensor array processing," *IEEE Transactions on Signal Processing*, vol. 48, pp. 2377–2388, 2000.
[35] J. B. Kruskal, "Rank decomposition, and uniqueness for 3-way and N-way arrays," in *Multi-way Data Analysis*, 1989, pp. 7–18.
[36] A. Toding, M. R. A. Khandaker, and Y. Rong, "Joint source and relay optimization for parallel MIMO relay networks," *EURASIP Journal on Advances in Signal Processing*, vol. 174, pp. 1–7, 2012.

André L. F. de Almeida (M'08–SM'13) received the double Ph.D. degree in Sciences and Teleinformatics Engineering from the University of Nice, Sophia Antipolis, France, and the Federal University of Ceará, Fortaleza, Brazil, in 2007. He is currently an Assistant Professor with the Department of Teleinformatics Engineering of the Federal University of Ceará. During fall 2002, he was a visiting researcher at Ericsson Research Labs, Stockholm, Sweden. From 2007 to 2008, he held a one year research position at the I3S Laboratory, CNRS, France. In 2008, he was awarded a CAPES/COFECUB research fellowship with the I3S Laboratory, CNRS, France. He currently holds a productivity research fellowship from CNPq (the Brazilian National Council for Scientific and Technological Development). In the spring 2012, he was a visiting professor at the University of Nice-Sophia Antipolis, France. He serves as an Associate Editor of the IEEE Transactions on Signal Processing. His research interests lie in the areas of signal processing for communications and sensor array processing, and include blind methods for channel identification, equalization and source separation, MIMO receivers, multilinear algebra and tensor-based signal processing applied to communications and data analysis.

Gérard Favier received the engineer diplomae from ENSCM (Ecole Nationale Supérieure de Chronométrie et de Micromécanique), Besançon, and ENSAE (Ecole Nationale Supérieure de l'Aéronautique et de l'Espace), Toulouse, the Dr.-Ing. (Ph.D.) and State Doctorate degrees from the University of Nice-Sophia Antipolis, France, in 1973, 1974, 1977 and 1981, respectively. In 1976, he joined the CNRS (French National Center for Scientific Research) and he is currently a Research Director of CNRS at the I3S Laboratory, in Sophia Antipolis, France. From 1995 to 1999, he was the Director of the I3S Laboratory. His research interests include nonlinear system modeling and identification, blind identification/equalization, tensor models/decompositions, and tensor approaches for MIMO communication systems. He is co-author or author of more than 200 papers published in international scientific conferences and journals, and 20 books or book chapters.

Leandro R. Ximenes received the B.Sc degree in electrical engineering from Federal University of Santa Catarina (UFSC), FlorianÃşpolis, Brazil, in 2009, and the M.Sc degree in Teleinformatics Engineering from the Federal University of Ceará (UFC), Fortaleza, Brazil, in 2011. He is currently working toward the double Ph.D degree at University of Nice-Sophia Antipolis, France and at Federal University of Ceará. During Fall 2010, he was a visiting researcher in the Sony Ericsson Mobile Communications, Lund, Sweden. His research interests are in the area of signal processing for wireless communications, including cooperative MIMO communications, blind channel estimation, tensor decompositions and adaptive filtering.